Novel application of three-dimensional shear wave elastography in the detection of clinically significant prostate cancer

SUNAO SHOJI[1], AKIO HASHIMOTO[2], TOMOYA NAKAMURA[2], SHINICHIRO HIRAIWA[3], HARUHIRO SATO[4], YOSHINOBU SATO[5], TAKUMA TAJIRI[3] and AKIRA MIYAJIMA[6]

Departments of [1]Urology, [2]Radiology and [3]Pathology, Tokai University Hachioji Hospital, Hachioji, Tokyo, 192-0032; [4]Department of Internal Medicine, Kanagawa Dental University, Yokosuka, Kanagawa 238-8580; [5]Imaging-based Computational Biomedicine Laboratory, Graduate School of Information Science, Nara Institute of Science and Technology, Ikoma, Nara 630-0192; [6]Department of Urology, Tokai University School of Medicine, Shimokasuya, Kanagawa 259-1193, Japan

Received September 9, 2017; Accepted November 16, 2017

DOI: 10.3892/br.2018.1059

Abstract. The present study evaluated three-dimensional shear wave elastography (3D SWE) in the detection of clinically significant prostate cancer. Clinically significant prostate cancer was defined by a minimum of one biopsy core with a Gleason score of 3+4 or 6 with a maximum cancer core length >4 mm. Patients with serum prostate-specific antigen levels of 4.0-20.0 ng/ml who were suspected of having prostate cancer from multi-parametric magnetic resonance imaging (mpMRI) were prospectively recruited. The 3D SWE was performed pre-biopsy, after which patients underwent MRI-transrectal ultrasound image-guided targeted biopsies for cancer-suspicious lesions and 12-core systematic biopsies. The pathological biopsy results were compared with the mpMRI and 3D SWE images. A total of 12 patients who were suspected of having significant cancer on mpMRI were included. The median pre-biopsy PSA value was 5.65 ng/ml. Of the 12 patients, 10 patients were diagnosed as having prostate cancer. In the targeted biopsy lesions, there was a significant difference in Young's modulus between the cancer-detected area (median 64.1 kPa, n=20) and undetected area (median 30.8 kPa, n=8; P<0.0001). On evaluation of receiver operating characteristics, a cut-off value of the Young's modulus of 41.0 kPa was used for the detection of clinically significant cancer, with which the sensitivity, specificity, positive predictive value (PPV) and negative predictive value (NPV) of cancer detection were 58, 97, 86 and 87%, respectively. When combining this cut-off tissue elasticity value with Prostate Imaging Reporting and Data System (PI-RADS) scores, the sensitivity, specificity, positive predictive value and negative predictive value of cancer detection were improved to 70, 98, 91 and 92%, respectively. In the cancer-detected lesions, a significant correlation was identified between the tissue elasticity value of the lesions and Gleason score (r=0.898, P<0.0001). In conclusion, PI-RADS combined with measurement of Young's modulus by 3D SWE may improve the diagnosis of clinically significant prostate cancer.

Correspondence to: Dr Sunao Shoji, Department of Urology, Tokai University Hachioji Hospital, 1838 Ishikawa-machi, Hachioji, Tokyo 192-0032, Japan
E-mail: sunashoj@mail.goo.ne.jp

Abbreviations: PCa, prostate cancer; SWE, shear wave elastography; 2D, two-dimensional; PSA, prostate-specific antigen; mpMRI, multi-parametric magnetic resonance imaging; US, ultrasound; 3D, three-dimensional; TRUS, transrectal ultrasound; DCE, dynamic contrast enhanced; PI-RADS, Prostate Imaging Reporting and Data System; ROC, receiver operating characteristic; Vs, shear wave velocity; APC, apparent diffusion coefficient; PPV, positive predictive value; NPV, negative predictive value; ROI, regions of interest; CI, confidence interval

Key words: prostate cancer, three-dimensional ultrasonography, shear wave elastography, magnetic resonance imaging, fusion image-guided biopsy, cancer detection, clinically significant cancer

Introduction

In the diagnosis of prostate cancer with ultrasound (US) imaging, gray scale US, Doppler US, dynamic contrast enhanced (DCE)-US and elastography have been widely used (1). The majority of prostate cancers are harder than normal prostatic tissue, due to increased micro-vascularity and a stromal response leading to increased collagen deposition around the tumor (2). Elastography evaluates tissue stiffness instead of echogenicity, which provides a novel method of detecting pathological abnormality that may otherwise be missed by conventional US (3). At present, there are two types of US elastography: Strain elastography and shear wave elastography (SWE) (4). Strain elastography requires user-applied uniform compression at the surface of the body to cause

deformation of the tissue. The US scanner then calculates and displays the induced deformation in the imaging plane. Due to its reliance on the individual applying pressure to the body, users have reported poor reproducibility and intra-operator variability with this method (4). Thus, in strain elastography, only relative information is obtained regarding the stiffness of the measured tissue, and it is not a quantitative imaging mode. By contrast, SWE provides a quantitative value of stiffness, thus yielding useful information of a pathological abnormality (4). Shear wave is a technique that uses a sonographic push pulse to generate a shear wave in the tissues. Shear wave velocity (V_s) through the tissue is affected by tissue stiffness, with stiffer tissues accommodating faster movement (5). Tissue stiffness may be expressed as Young's modulus or as the ratio of stress on a material to the tissue deformation caused by the stress (6). The V_s or Young's modulus (kPa) for each pixel is color-coded and overlaid on a B-mode image (7). The SWE, or tissue elasticity, is detected by tissue response to an operator-independent compression wave pulsed into the tissue by an ultrasound probe (7). Woo *et al* (8) reported that the intra-observer reproducibility of SWE in terms of Young's modulus (kPa) was high [intraclass correlation coefficients =0.876, 95% confidence interval (CI) =0.864-0.887]. Barr *et al* (9) reported that a value of 37 kPa may be used as a cut-off between benign and malignant prostate tissue on the basis of the receiver operating characteristic (ROC) curve. This achieved a sensitivity of 96.2%, a specificity of 96.2%, a positive predictive value (PPV) of 69.4%, and a negative predictive value (NPV) of 99.6% in 318 sextants from 53 patients (9). Furthermore, this method was more sensitive and specific in diagnosing the prostate cancer than strain elastography (9).

Recently, clinically significant prostate cancer, defined by at least one biopsy core with a Gleason score of 3+4 or 6 with a maximum cancer core length greater than 4 mm, has been considered to be associated with cancer progression (10). In the detection of significant prostate cancer, multi-parametric magnetic resonance imaging (mpMRI) is becoming more used due to its increased availability and capacity to combine anatomical and functional data (11,12). To standardize the evaluation and reporting of MRI findings of the prostate, the European Society of Urogenital Radiology published guidelines, termed the Prostate Imaging Reporting and Data System (PI-RADS) (13). In this system, suspicious areas, known as 'regions of interest (ROI)', are defined and radiologists provide a likelihood score that clinically significant cancer is present for each ROI from 1 to 5 on the PI-RAD classification14: 1, most probably benign; 2, probably benign; 3, intermediate; 4, probably malignant; 5, highly suspicious of malignancy (13,14). In a diagnostic meta-analysis of the standardized evaluation system of PI-RADS, the sensitivity and specificity for pooled studies were 78% (95% CI: 70-84) and 79% (95% CI: 68-86), respectively (15). Although mpMRI findings may be useful for detecting significant prostate cancer, the differential diagnosis of certain prostate cancers from benign prostatic hyperplasia and inflammation is challenging in mpMRI, as the signal intensity of these lesions can be similar to that of the tumor tissue (16). Therefore, elastography may be more effective, as a separate technique to mpMRI, in the detection of significant prostate cancer.

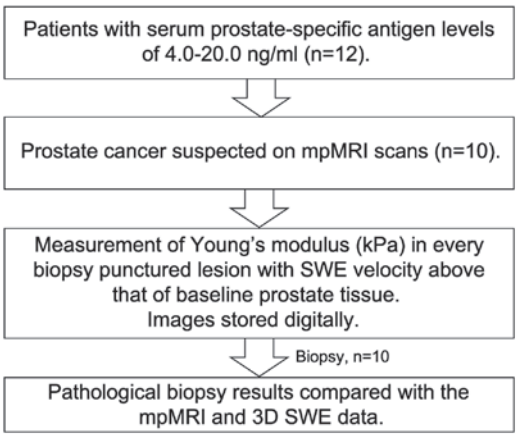

Figure 1. Diagnostic procedure. Of the 12 patients, 10 patients were diagnosed with prostate cancer on mpMRI. Measurement of Young's modulus (kPa) was performed in every biopsy punctured lesion with SWE velocity above that of the baseline prostate tissue. Images were stored digitally. The pathological biopsy results were compared with the mpMRI and 3D SWE imaging data. mpMRI, multi-parametric magnetic resonance imaging; 3D SWE, three-dimensional shear wave elastography.

The development of three-dimensional (3D) US has enabled 3D visualization of the prostate, allowing diagnosis and localization of prostatic lesions. In the present study, the applications of 3D SWE in the detection of significant prostate cancer were evaluated. To the best of our knowledge, the current study is the first to determine the efficacy of 3D SWE in the detection of significant prostate cancer.

Materials and methods

Study population. The study prospectively recruited patients with serum prostate specific antigen (PSA) levels of 4.0-20.0 ng/ml who were suspected of having prostate cancer from mpMRI scans taken from May 2016 to June 2016 at Tokai University Hachioji Hospital (Tokyo, Japan). The study was approved by the Institutional Review Board for Clinical Research of Tokai University School of Medicine (Shimokasuya, Japan) and informed consent was obtained from all patients prior to enrollment.

mpMRI. MRI examination was conducted as described in our previous study (17). Briefly, the MRI examination was performed using a 1.5-Tesla magnet (Signa HDx®; GE Healthcare Life Sciences, Little Chalfont, UK) with an 8-channel cardiac coil. T1-weighted fat-saturated axial fast spin-echo images [repetition time (TR), 450 ms; echo time (TE), 8.8 ms; slice thickness, 3 mm; resolution, 0.9x1.3 mm] were obtained prior to injection. An intravenous bolus of 0.2 ml/kg meglumine gadopentetate (Magnevist Syringe®; Bayer AG, Leverkusen, Germany) was then injected. All MRI examinations were performed using the same protocol, and included non-enhanced T2-weighted images (TR, 5,000 ms; TE, 125 ms; slice thickness, 3 mm; resolution, 0.6x0.9 mm) acquired in the axial and sagittal planes, diffusion weighted images and apparent diffusion coefficient (ADC) maps (b-value =1,500 s/mm^2), and DCE imaging (resolution, 0.9x1.3 mm) using a fat-saturated T1-weighted fast-field echo sequence

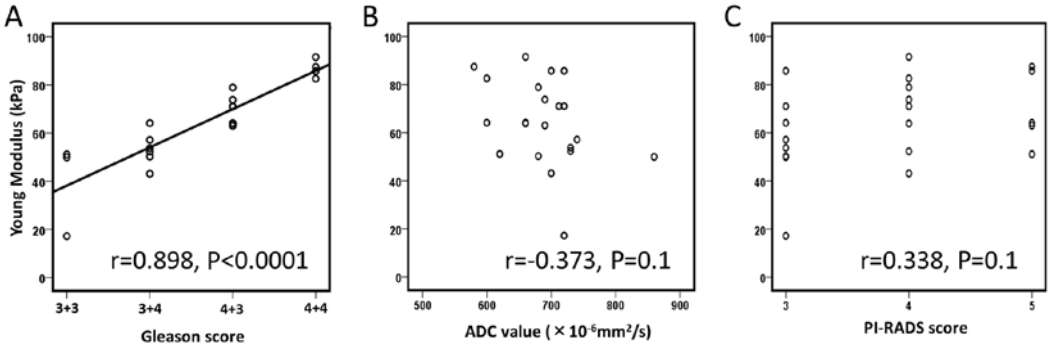

Figure 2. Associations of tissue elasticity value with (A) Gleason score, (B) ADC value and (C) PI-RADS score for lesions diagnosed with prostate cancer. A significant association was identified between the tissue elasticity value and Gleason score, while there was no association between the tissue elasticity value and ADC value (P=0.1) or PI-RADS score (P=0.1). ADC, apparent diffusion coefficient; PI-RADS, Prostate Imaging Reporting and Data System.

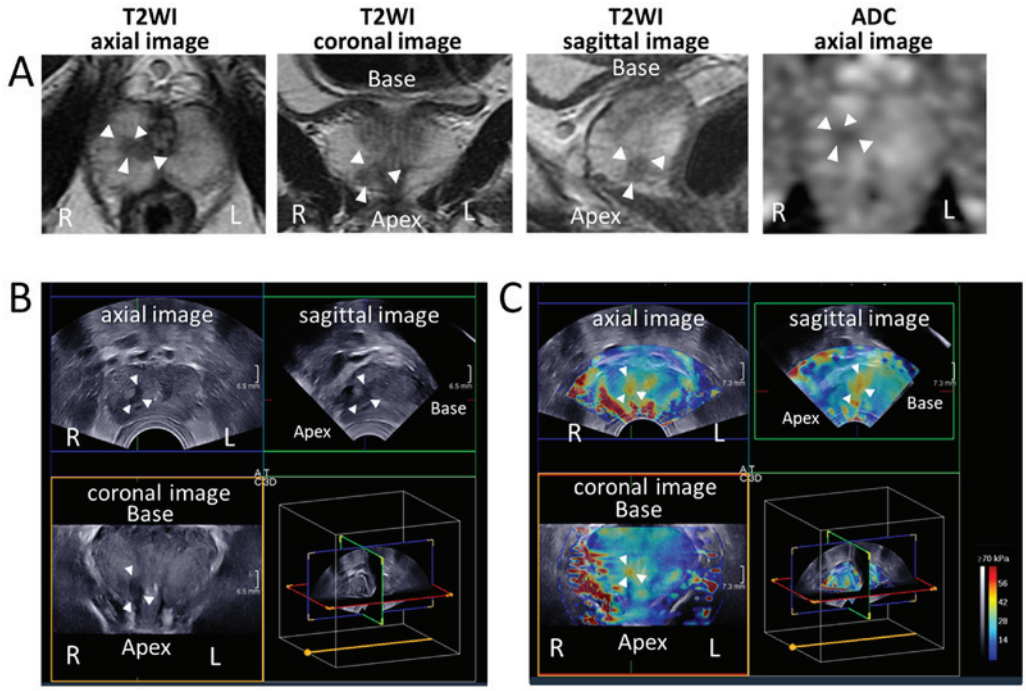

Figure 3. Representative images of mpMRI, 3D gray scale TRUS and 3D SWE scans of patients. (A) MRI, (B) 3D gray scale TRUS and (C) 3D SWE images of the prostate in a patient determined to have clinically significant cancer on mpMRI. White arrowheads indicate the cancer-suspected lesion. The tissue elasticity value of the lesion was 43.1 kPa, and pathological examination of biopsy specimens from the lesion indicated adenocarcinoma of Gleason score 3+3=6. mpMRI, multi-parametric magnetic resonance imaging; TRUS, transrectal ultrasound; SWE, shear wave elastography; 3D, three-dimensional; T2WI, T2-weighted image; ADC, apparent diffusion coefficient; R, right; L, left.

in the axial plane. All mpMRI images were reviewed by two experienced radiologists with no prior clinical information. Suspicious areas, or ROIs, were defined and the radiologists provided a likelihood score that clinically significant cancer was present for each ROI from 1 to 5 on the PI-RADS (14): 1, most probably benign; 2, probably benign; 3, intermediate; 4, probably malignant; 5, highly suspicious of malignancy (13,14).

3D SWE. At pre-biopsy, 3D SWE was performed using the Aixplorer® equipped with an SE12-3 146° Super Endocavity Volumetric Array (SuperSonic Imagine, Aix-en-Provence, France) on patients in lithotomy position under spinal anesthesia with 1.2 ml high specific gravity type 0.5% marcaine (Aspen Japan K.K., Tokyo, Japan). The minimum amount of pressure on the prostate was applied while maintaining contact with the probe. For each imaging procedure, the probe was held steady for 30 sec. Measurement of Young's modulus was performed in all biopsy-punctured lesions with SWE Vs above that of the baseline prostate tissue. Images were stored digitally.

MRI-TRUS fusion image-guided prostate biopsy. MRI-TRUS fusion image-guided prostate biopsy was performed with a BioJet® system version 2.0 (D&K Technologies GmbH, Barum, Germany). The biopsy was performed as described previously (17). Targeted biopsies for cancer-suspicious lesions were initially performed, followed by 12-core systematic biopsies, using the transperineal method. Immediately after each biopsy, the spatial punctured needle orbits were recorded in the 3D model reconstructed from MRI.

Pathological analysis. All biopsy samples were examined by two senior pathologists in cohesion. Clinically significant cancer was defined as follows: A minimum of one core with a Gleason score (18) of 3+4 or 6 with a maximum cancer core length >4 mm (10). The pathological biopsy results were compared with the images from mpMRI and 3D SWE.

Statistical analysis. All statistical analyses were performed using IBM SPSS® software version 19.0 (IBM Corp., Armonk, NY, USA). For the detected and un-detected lesions by biopsy, the difference in median tissue elasticity values was analyzed using the Mann-Whitney U-test. The association between Young's modulus, mpMRI data and pathological findings for the cancer-detected lesions was assessed by Pearson correlation. P<0.05 was considered to indicate statistically significant differences. Young's modulus was evaluated in the detection of prostate cancer using ROC analyses.

Results

Patient characteristics and cancer detection by mpMRI. A total of 12 patients were included in the present study. The patient characteristics are presented in Table I. The median age of the patients was 65 years (range, 49-78). The median pre-biopsy PSA value was 5.65 ng/ml (range, 4.14-10.91). The median prostate volume was 28 ml (range, 22-32). The median number of biopsies for each patient was 13 cores (range, 13-15). The median number of targeted biopsies for each patient was 2 cores (range, 1-3). The diagnostic procedure is depicted in Fig. 1. Of the 12 patients, 10 patients were diagnosed with prostate cancer by mpMRI. The median lengths of the maximum and minimum diameters of the cancer-detected lesions on T2-weighted image MRI were 10.2 mm (range, 4.8-24.0) and 5.8 mm (range, 3.0-12.0), respectively. Using mpMRI, 28 suspected cancer lesions were diagnosed, comprising of 13 lesions of PI-RADS score 3, 10 lesions of PI-RADS score 4and 5 lesions of PI-RADS score 5. Cancer diagnosis was confirmed for 21 of the 28 lesions (75%), including 62% (8/13) of the lesions with PI-RADS score 3, 80% (8/10) of the lesions with PI-RADS score 4 and 100% (5/5) of the lesions with PI-RADS score 5. The sensitivity, specificity, PPV and NPV of cancer detection based on PI-RADS score ≥3 were 70, 94, 75 and 92%, respectively.

Cancer detection by 3D SWE and mpMRI. Using 3D SWE, all of the suspected cancer lesions assessed by mpMRI were detected and measured for tissue elasticity value. The median tissue elasticity value for the cancer-detected areas was significantly higher compared with that of the undetected areas [63.6 kPa (range, 18.8-85.7) vs. 24.1 kPa (range 5.8-58.9), P<0.0001]. Similarly, in the targeted biopsy lesions, tissue elasticity was significantly higher in the cancer-detected areas (median 64.1, range 17.2-91.5, n=20) compared with the undetected areas (median 30.8, range 11.2-38.8, n=8), respectively (P<0.0001; data not shown). On ROC analysis, the cut-off value of the Young's modulus was determined to be 41.0 kPa for the detection of clinically significant cancer, with which the sensitivity, specificity, PPV and NPV of cancer detection were 58, 97, 86 and 87%, respectively. When this value for Young's modulus was used in conjunction with PI-RADS score, the cancer detection rates in suspected cancer lesions (PI-RADS score ≥3) with Young's modulus >41.0 kPa and <41.0 kPa were 91% (21/23 lesions) and 0% (0/5 lesions), respectively. Thus, by combining the cut-off value of Young's modulus with PI-RADS score, cancer was diagnosed in 21 of 23 lesions (91%), including 89% (8/9) of the lesions with PI-RADS score 3, 89% (8/9) of the lesions with PI-RADS score 4 and 100% (5/5) of the lesions with PI-RADS score 5. Furthermore, when combining the cut-off value of Young's modulus with PI-RADS score, the sensitivity, specificity, PPV and NPV of cancer detection in confirmed cancer lesions were 70, 98, 91 and 92%, respectively (data not shown). In these cancer-detected lesions, a significant association was identified between the tissue elasticity value of the lesions and Gleason score (r=0.898, P<0.0001); however, there was no association between the tissue elasticity value of the lesions with ADC value (r=-0.373, P=0.1) or PI-RADS score (r=0.338, P=0.1), respectively (Fig. 2). Fig. 3 depicts representative images of the mpMRI, TRUS and 3D SWE scans performed on patients.

Table I. Patient characteristics.

Variable	Value
Median age, years (range)	65 (49-78)
Median prostate-specific antigen, ng/ml (range)	5.65 (4.14-10.91)
Median prostate volume, ml (range)	28 (22-32)
Median number of biopsies for each patient, n (range)	13 (13-15)
Median number of targeted biopsies for each patient, n (range)	2 (1-3)
Median length of maximum diameter of cancer-detected lesions on T2WI MRI, mm (range)	10.2 (4.8-24.0)
Median length of minimum diameter of cancer-detected lesions on T2WI MRI, mm (range)	5.8 (3.0-12.0)

T2WI MRI, T2-weighted image magnetic resonance imaging.

Discussion

SWE evaluates tissue elasticity, or Vs, by using a sonographic push pulse to generate a shear wave in the tissues; Vs through the tissue is affected by tissue stiffness, with stiffer tissues accommodating faster movement (5). Previous reports have indicated the clinical applications of SWE (19,20). Ahmad *et al* (19) reported that data analyzed per core regarding SWE findings indicated that for patients with serum PSA <20 ng/ml, the sensitivity and specificity of SWE for prostate cancer detection were 90 and 88%, respectively, while in patients with PSA >20 ng/ml, the sensitivity and specificity were 93 and 93%, respectively. Correas *et al* (20) reported that the sensitivity, specificity, PPV, NPV and AUC for SWE with a cut-off of 35 kPa for differentiating benign from malignant

lesions in 1,040 peripheral zone sextants from 184 patients were 96% (95% CI: 95-97), 85% (95% CI: 83-87), 48% (95% CI: 46-50), 99% (95% CI: 98-100) and 95% (95% CI: 93-97), respectively. In the present study, when combining the cut-off value of 41.0 kPa for tissue elasticity to PI-RADS score, the sensitivity, specificity, PPV and NPV of cancer detection were 70, 98, 91 and 92%, respectively. Based on these results, 3D SWE may have potential for improving the detection of significant prostate cancer.

Although the majority of prostate cancers are harder than normal prostatic tissue (2), elastography is not included in mpMRI. The applications of elastography in the detection of significant prostate cancer was evaluated using 3D SWE in the present study. In a previous report on SWE, it was observed that prostate cores with a Gleason score of 7 had a higher mean Young's modulus (163±63 kPa) compared with cores with a Gleason score of 6 (95±28.5 kPa; P=0.007) (19). Similarly, Woo *et al* (21) reported that Young's modulus was significantly correlated with Gleason score (r=0.343, P=0.002). In the present study, a significant association was identified between the tissue elasticity value of prostatic lesions and Gleason score (r=0.898, P<0.0001), while there were no associations between the tissue elasticity value and ADC value (P=0.1) or PI-RADS score (P=0.1). Additionally, there was no significant association between ADC value and Gleason score in the cancer-detected lesions in the present series (P=0.1). These results indicate the potential of Young's modulus to predict Gleason scores more accurately compared with ADC value, possibly due to the different approach of measuring the targeted lesion.

The current study had several limitations. First, it was a single-institutional study and patients were not randomized to facilitate comparison of biopsy techniques. Furthermore, although previous reports have demonstrated high reproducibility of SWE (8), a single operator performed the 3D SWE in the present study. Therefore, a multi-institutional randomized study is now required to confirm the efficacy of the biopsy methods. Second, the study lacked a comparison of biopsy results and pathological findings of whole-gland specimens. Therefore, although the locations and pathological grades of clinically significant cancers corresponded to the results of the targeted biopsies, it is possible that a clinically significant cancer was omitted in the absence of large-scale pathological analysis of whole-gland specimens.

In conclusion, the tissue elasticity values of cancer-detected areas were significantly higher compared with those of undetected areas (P<0.0001), and PI-RADS combined with measurement of Young's modulus by 3D SWE may have potential for improving the diagnosis of clinically significant prostate cancer. However, additional multi-institutional studies are now required to validate the usefulness of 3D SWE in detecting clinically significant prostate cancer.

References

1. Postema A, Mischi M, de la Rosette J and Wijkstra H: Multiparametric ultrasound in the detection of prostate cancer: A systematic review. World J Urol 33: 1651-1659, 2015.
2. Good DW, Stewart GD, Hammer S, Scanlan P, Shu W, Phipps S, Reuben R and McNeill AS: Elasticity as a biomarker for prostate cancer: A systematic review. BJU Int 113: 523-534, 2014.
3. Aigner F, Pallwein L, Schocke M, Lebovici A, Junker D, Schäfer G, Mikuz G, Pedross F, Horninger W, Jaschke W, *et al*: Comparison of real-time sonoelastography with T2-weighted endorectal magnetic resonance imaging for prostate cancer detection. J Ultrasound Med 30: 643-649, 2011.
4. Correas JM, Tissier AM, Khairoune A, Khoury G, Eiss D and Hélénon O: Ultrasound elastography of the prostate: State of the art. Diagn Interv Imaging 94: 551-560, 2013.
5. Nelson ED, Slotoroff CB, Gomella LG and Halpern EJ: Targeted biopsy of the prostate: The impact of color Doppler imaging and elastography on prostate cancer detection and Gleason score. Urology 70: 1136-1140, 2007.
6. Ophir J, Garra B, Kallel F, Konofagou E, Krouskop T, Righetti R and Varghese T: Elastographic imaging. Ultrasound Med Biol 26 (Suppl 1): S23-S29, 2000.
7. Mitri FG, Urban MW, Fatemi M and Greenleaf JF: Shear wave dispersion ultrasonic vibrometry for measuring prostate shear stiffness and viscosity: An in vitro pilot study. IEEE Trans Biomed Eng 58: 235-242, 2011.
8. Woo S, Kim SY, Lee MS, Cho JY and Kim SH: Shear wave elastography assessment in the prostate: An intraobserver reproducibility study. Clin Imaging 39: 484-487, 2015.
9. Barr RG, Memo R and Schaub CR: Shear wave ultrasound elastography of the prostate: Initial results. Ultrasound Q 28: 13-20, 2012.
10. Harnden P, Naylor B, Shelley MD, Clements H, Coles B and Mason MD: The clinical management of patients with a small volume of prostatic cancer on biopsy: What are the risks of progression? A systematic review and meta-analysis. Cancer 112: 971-981, 2008.
11. Vilanova JC, Barceló-Vidal C, Comet J, Boada M, Barceló J, Ferrer J and Albanell J: Usefulness of prebiopsy multifunctional and morphologic MRI combined with free-to-total prostate-specific antigen ratio in the detection of prostate cancer. AJR Am J Roentgenol 196: W715-22, 2011.
12. Delongchamps NB, Rouanne M, Flam T, Beuvon F, Liberatore M, Zerbib M and Cornud F: Multiparametric magnetic resonance imaging for the detection and localization of prostate cancer: Combination of T2-weighted, dynamic contrast-enhanced and diffusion-weighted imaging. BJU Int 107: 1411-1418, 2011.
13. Barentsz JO, Richenberg J, Clements R, Choyke P, Verma S, Villeirs G, Rouviere O, Logager V and Fütterer JJ; European Society of Urogenital Radiology: ESUR prostate MR guidelines 2012. Eur Radiol 22: 746-757, 2012.
14. Röthke M, Blondin D, Schlemmer HP and Franiel T: PI-RADS classification: Structured reporting for MRI of the prostate. Rofo 185: 253-261, 2013 (In German).
15. Hamoen EHJ, de Rooij M, Witjes JA, Barentsz JO and Rovers MM: Use of the Prostate Imaging Reporting and Data System (PI-RADS) for Prostate Cancer Detection with Multiparametric Magnetic Resonance Imaging: A Diagnostic Meta-analysis. Eur Urol 67: 1112-1121, 2015.
16. Oto A, Kayhan A, Jiang Y, Tretiakova M, Yang C, Antic T, Dahi F, Shalhav AL, Karczmar G and Stadler WM: Prostate cancer: Differentiation of central gland cancer from benign prostatic hyperplasia by using diffusion-weighted and dynamic contrast-enhanced MR imaging. Radiology 257: 715-723, 2010.
17. Shoji S, Hiraiwa S, Ogawa T, Kawakami M, Nakano M, Hashida K, Sato Y, Hasebe T, Uchida T and Tajiri T: Accuracy of real-time magnetic resonance imaging-transrectal ultrasound fusion image-guided transperineal target biopsy with needle tracking with a mechanical position-encoded stepper in detecting significant prostate cancer in biopsy-naïve men. Int J Urol 24: 288-294, 2017.
18. Gleason DF, Mellinger GT, Arduino LJ, Bailar JC III, Becker LE III, Berman HI III, Bischoff AJ, Byar DP, Blackard CE, Doe RP, *et al*: Prediction of prognosis for prostatic adenocarcinoma by combined histological grading and clinical staging. J Urol 111: 58-64, 1974.
19. Ahmad S, Cao R, Varghese T, Bidaut L and Nabi G: Transrectal quantitative shear wave elastography in the detection and characterisation of prostate cancer. Surg Endosc 27: 3280-3287, 2013.
20. Correas JM, Tissier AM, Khairoune A, Vassiliu V, Méjean A, Hélénon O, Memo R and Barr RG: Prostate cancer: Diagnostic performance of real-time shear-wave elastography. Radiology 275: 280-289, 2015.
21. Woo S, Kim SY, Cho JY and Kim SH: Shear wave elastography for detection of prostate cancer: A preliminary study. Korean J Radiol 15: 346-355, 2014.